Warm plasma activation of CO_2 in a rotating gliding arc discharge reactor

Hao Zhang[a], Li Li[a], Xiaodong Li [a,*], Weizong Wang[b], Jianhua Yan[a], Xin Tu[c,*]
[a] *State Key Laboratory of Clean Energy Utilization, Zhejiang University, Hangzhou 310027, China*
[b] *School of Astronautics, Beihang University, Beijing 100191, China*
[c] *Department of Electrical Engineering and Electronics, University of Liverpool, Liverpool L69 3GJ, UK*

Abstract:

In this study, a rotating gliding arc (RGA) warm plasma has been developed for the conversion of CO_2 into CO and O_2. The effect of feed flow rate, applied voltage, arc current, and the addition of N_2 or Ar on the reaction performance has been investigated. The results show two variation patterns of CO_2 conversion and energy efficiency, depending on the specific energy input (SEI): In Pattern A with SEI > 3.5 kJ/L, the CO_2 conversion and energy efficiency decrease simultaneously with increasing SEI, while in Pattern B with SEI ≤ 3.5 kJ/L, the energy efficiency and the CO_2 conversion show an opposite trend. The recombination of CO and O at high temperatures could be responsible for the decrease of CO_2 conversion with rising SEI due to the increased retention time or gas temperature. A CO_2 conversion of 4.0-4.4% and energy efficiency of 16-17% can be achieved. Compared to other non-thermal plasmas, the RGA plasma exhibits a lower CO_2 conversion but higher energy efficiency, whilst maintaining a flow rate (e.g, 6-7 L/min) that is significantly higher than that of typical non-thermal plasmas (e.g., 20-125 ml/min in dielectric barrier and corona discharges). Increasing the fraction of N_2 or Ar promotes the conversion of CO_2 but lowers the energy efficiency. N_2 is clearly more beneficial for enhancing the CO_2 conversion in comparison to Ar. Further enhancement of the reaction performance can be expected by cooling the plasma area to lower the gas temperature, to limit the recombination of CO and O.

Keywords: CO_2 dissociation; rotating gliding arc; warm plasma; flow rate; specific energy input

1. Introduction

In the Synthesis Report of Climate Change 2014, the Intergovernmental Panel on Climate Change (IPCC) confirmed that human influence on the climate change is clear, and recent anthropogenic emissions of greenhouse gases reach the highest on record [1]. The atmospheric concentration of the

* *Corresponding authors.* Tel.: +86 571 87952037 (X. D. Li), +44-1517944513 (X. Tu).
E-mail addresses: lixd@zju.edu.cn (X. D. Li), xin.tu@liverpool.ac.uk (X. Tu)

major greenhouse gas CO_2 has been increasing from a preindustrial level of 280 ppm to an unprecedented level of 400 ppm in 2014 [1]. Undoubtedly, the development of effective strategies for the mitigation and valorization of CO_2 has been of unprecedented importance. Significant efforts have been devoted to these strategies, such as boosting the use of clean and renewable energy, improving energy utilization efficiency, carbon capture and storage (CCS), as well as carbon capture and utilization (CCU) [2]. Among these strategies, the conversion of CO_2 into value-added chemicals or fuels has been considered as one of the attractive solutions for CO_2 reduction, which not only complies with the framework of sustainable and green chemistry but also fits within the 'cradle-to-cradle' concept (an ecologically intelligent concept focusing on closed-loop cycles of production, recovery and remanufacture) [3]. Several chemical processes have been investigated in this regard, including CO_2 reforming of CH_4 and CO_2 hydrogenation with H_2, aiming for the production of syngas and value-added oxygenates (e.g., methanol, formic acid, and formaldehyde) [3]. Direct dissociation of CO_2 into CO (eq. (1)) is also of particular interest [3-6], because CO is an important chemical feedstock for the production of a range of platform chemicals (e.g., organic acid and aldehyde etc. [7]) and synthetic fuels (e.g., via Fischer-Tropsch process [4]).

$$CO_2 \rightarrow CO + \frac{1}{2}O_2 \qquad \Delta H = 280\ \text{kJ/mol} \tag{1}$$

However, CO_2 is a highly stable molecule and its activation remains a challenge as a large amount of energy is required for CO_2 conversion in a traditional thermal process. Thermodynamic equilibrium calculation of this reaction shows that CO_2 begins to split at near 2000 K with a fairly low conversion of <1% [5]. In this regard, non-thermal plasma has emerged as an attractive alternative solution for the effective decomposition of CO_2 as it enables this thermodynamically unfavourable reaction (i.e., CO_2 activation) to proceed with a reduced energy cost under mild conditions, i.e., lower temperature and atmospheric pressure [3, 8, 9]. In non-thermal plasmas, the electrical energy is selectively applied to producing highly energetic electrons with a typical average electron energy of 1-10 eV, which can directly activate inert gas molecules (e.g., CO_2) to generate highly reactive species (e.g., excited species, radicals, ions, and photons) for the initiation and propagation of plasma chemical reactions [10, 11]. In the meantime, the gas kinetic temperature of non-thermal plasmas remains relatively low [12-14]. Furthermore, the compactness (high specific productivity) and flexibility (high reaction rate, instantaneous 'on-and-off') of non-thermal plasma systems offers a promising solution to the imbalance between energy production and consumption by intermittent renewable sources, e.g., solar and wind, creating a carbon-neutral network [15-17].

Various non-thermal plasma systems have been reported in the literature for direct dissociation of CO_2, among which dielectric barrier discharge (DBD) [5, 6, 8, 16, 18-23], microwave (MW) discharge [24-28] and gliding arc discharge [29-34] are the most commonly investigated types. It is known that the vibrational excitation of CO_2 is the most efficient way for the dissociation of CO_2 to CO [10]. In DBD plasmas, the conversion of CO_2 has been demonstrated to be dominated by electron-impact excitation followed by dissociation and the vibrational excitation of CO_2 is found to be of minor importance, thus typically showing a limited energy efficiency of $<10\%$ [3]. MW discharges can enable an efficient dissociation of CO_2 via the vibrational excitation pathway (e.g., conversion of 30% and energy efficiency of 40% [24]), but was only achieved at a reduced pressure (50-200 torr), which is undoubtedly not desirable from an industrial application point of view.

In this regard, gliding arc discharge is among the most promising plasmas because it offers the possibility to operate at atmospheric pressure and simultaneously reach a non-equilibrium state that is strong enough to stimulate the most efficient dissociation of CO_2 through vibrational excitation [3]. In addition, gliding arc discharge can provide a significantly higher energy density and electron energy in comparison to other non-thermal plasmas (e.g., DBD), providing high flexibility to work in a wide range of reactant flow rates and plasma power levels (up to several kW) [10, 35]. However, in a traditional flat gliding arc reactor that consists of two divergent electrodes [36], the flow rates are normally limited to a high value (e.g., 10-20 L/min) for the formation and maintenance of gliding arc, which consequently results in a fairly short retention time of reactant [3, 37-40]. More importantly, although out-of-plane motion exists in the gliding arc [39, 41], the plasma reaction area that confined by the flat electrodes leads to a limited fraction of the gas flow that processed by the plasma (e.g., around 20% depending on the reactor geometry) [3, 42].

To overcome these problems, a direct current (DC) rotating gliding arc (RGA) co-driven by a magnetic field and tangential flow has been developed in our previous studies [43, 44]. The rotating of gliding arc can be driven by tangential flow, e.g., in the work by Lee et al. [45, 46], or by magnetic field, e.g., in the work by Fridman et al. [13, 47]. Whereas, the RGA plasma used in this work can provide a synergistic effect of the Lorentz force and swirling flow, ensuring the generation of a more stable plasma area with a higher rotation speed (up to 120 rotations per second) even at a very low gas flow rate (e.g., 0.1 L/min). In addition, the RGA plasma has been evidenced to be a kind of warm plasma, which shows transitional properties between thermal and typical non-thermal plasmas, with an electron temperature of around 1 eV, a relatively high gas temperature of 1300-2000 K, a high discharge power of 200-400 W, as well as a high electron density of 10^{13}-10^{15} cm^{-3} [37, 44, 48]. The RGA warm plasma is potentially promising for energy-efficient CO_2 activation because the electron energy of around 1 eV is ideal for the vibrational excitation of CO_2 molecules [10, 29, 31], which is the most energy efficient pathway for CO_2 dissociation. The optical emission spectroscopy (OES) results showed that the RGA plasmas in CH_3OH/N_2 has a CN vibrational temperature of up to 9000 K [37], which is considerably higher than that of other typical non-thermal plasmas, e.g., DBD in N_2 or Ar (2000-5000K) [49-52], indicating that the RGA plasma allows a high level of vibrational excitation. Moreover, the high electron density and discharge power of the RGA plasma enable an efficient reactor productivity, as demonstrated in our previous studies [42, 44]. In this study, we report the dissociation of CO_2 using a DC RGA warm plasma co-driven by a magnetic field and tangential flow for the first time, with specific emphasis on the investigation of the effect of feed flow rate, applied voltage, and arc current on the reaction performance of the plasma process. Additionally, N_2 or Ar is added into the RGA CO_2 plasma to understand the effect of additive gases on the reaction performance.

2. Experimental setup and methods

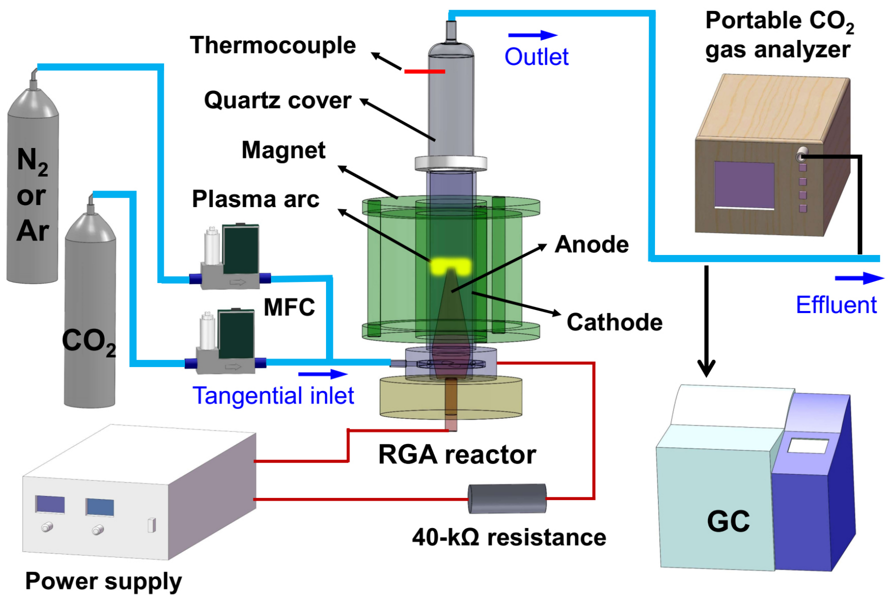

Fig. 1 Schematic diagram of the experimental setup

The schematic diagram of the experimental setup is shown in Fig. 1. The RGA reactor consists of a cone-shaped inner anode that connected to a high-voltage source and a circular cathode that is grounded. The plasma was powered by a customized 10 kV DC power supply (TLP2040, Teslaman) which can serve as either a constant voltage source or constant current source. A 40 kΩ resistance was connected in series in the circuit to limit and stabilize the current. The reactant gas CO_2 (and additive gases) was injected via three tangential inlets at the bottom of the reactor to form a swirling flow inside the reactor. An annular magnet is placed outside of the cathode, generating an upward magnetic field for the stabilization and acceleration of the arc. With the combined effect of swirling flow and Lorentz force, the arc moves upward and finally rotates rapidly around the inner anode, forming a stable plasma volume for chemical reactions (see Fig. 2 and Fig. 3). A more detailed description of the RGA reactor can be found in our previous work [44].

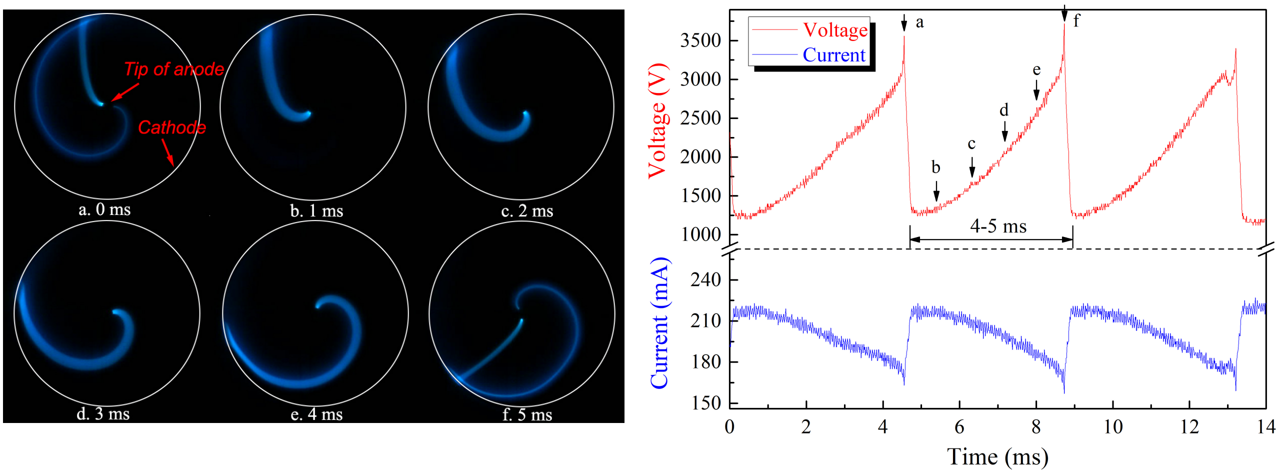

(1) (2)

Fig. 2 (1) High-speed frames of the plasma arcs (1000 frames/s, exposure time = 500μs) and (2) the corresponding electrical signals (feed flow rate = 6 L/min)

Fig. 2 presents the motion behavior and electrical characteristics of the RGA plasma. Clearly, the first arc initially forms at the shortest gap between the anode and cathode. Under the synergistic effect of swirling flow and Lorentz force, the formed arc is pushed up gradually to the tip of the inner anode, where it finally rotates rapidly and steadily, as shown in Fig. 2(1). A rotating cycle of the arc starts from frame (a), where a long arc is replaced by a shorter new arc between the electrodes. In the meantime, the discharge voltage drops suddenly to a minimum value (point a in Fig. 2(2)), with a rate of 11-13 kV/ms. Afterwards, the new arc rotates around the tip of the anode with a gradual increase in the arc length, as clearly seen in frames (b)-(e). The arc length for frames (a)-(e) is calculated to be 18.6, 22.6, 30.3, 39.7, and 50.5 mm, respectively. The discharge voltage is positively correlated with the arc length [53] and thus increases with the elongation of the arc (see points b-e in Fig. 2(2)). It is clear that a new rotating cycle repeats starting from frame (f) (point f in Fig. 2(2)), where the arc length and the associated discharge voltage reaches a peak value and is subsequently followed by the formation of a shorter discharge channel (a sudden drop). The rotating period (waveform period) is around 4-5 ms.

A thermocouple was placed at 6 cm vertically above the plasma area to measure the outlet gas temperature. The CO_2 concentration was detected online by a portable infrared CO_2 gas analyzer (GXH-3010E1, Huayun Instrument). The gaseous products were measured by a gas chromatograph (GC) (GC9790A, Fuli Analytical Instrument) equipped with a thermal conductivity detector (TCD) for detecting O_2 and a flame ionization detector (FID, with catalytic methanation) for detecting CO. Each experiment was repeated three times with similar results. Fig. 3 shows the time evolution of CO_2 concentration with and without plasma.

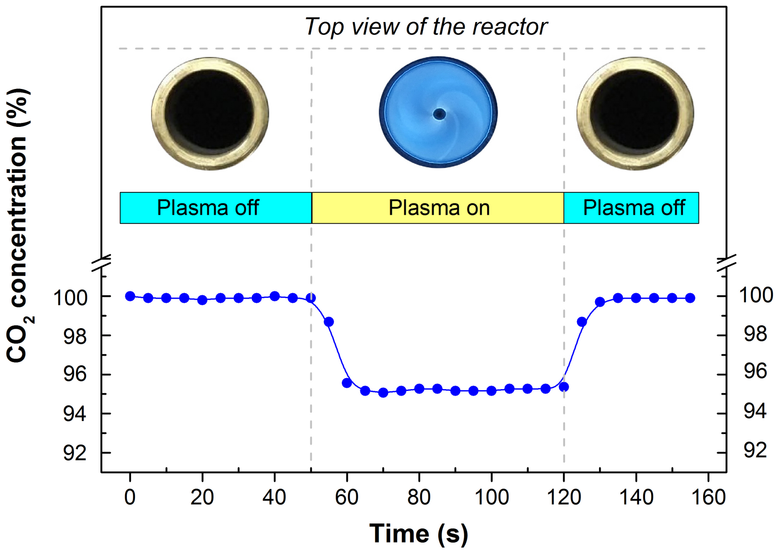

Fig. 3 Time dependent variation of the CO_2 concentration in the experiment (applied voltage = 10 kV; CO_2 flow rate= 5.9 L/min)

For the CO_2 dissociation process, the CO_2 conversion (X) and carbon balance (B) were defined as:

$$X(CO_2)\ (\%)=\frac{CO_2\ \text{converted (mol/min)}}{CO_2\ \text{introduced (mol/min)}}\times 100\% \quad (2)$$

$$B(\text{carbon})\ (\%)=\frac{CO_2\ \text{output (mol/min)} + CO\ \text{produced (mol/min)}}{CO_2\ \text{introduced (mol/min)}}\times 100\% \quad (3)$$

The specific energy input (*SEI*) was defined to represent the energy density applied to the plasma reaction area.

$$SEI\,(\text{kJ/L})=\frac{\text{Dishcharge power (W)}\times 60/1000}{\text{Feed flow rate (L/min)}} \quad (4)$$

The discharge power was calculated as the product of discharge voltage and current.

To indicate how efficiently the plasma process performs compared to the standard reaction enthalpy (ΔH), the energy efficiency (η) was calculated based on the following equation.

$$\eta(\%)=\frac{CO_2\ \text{feed flow rate (mol/min)} \times X(CO_2)\ (\%) \times \Delta H\,(\text{kJ/mol})}{\text{Discharge power (W)} \times 60/1000} \quad (5)$$

As shown in eq. (1), ΔH is 280 kJ/mol for pure CO_2 splitting process.

3. Results and Discussion

3.1 Effect of feed flow rate

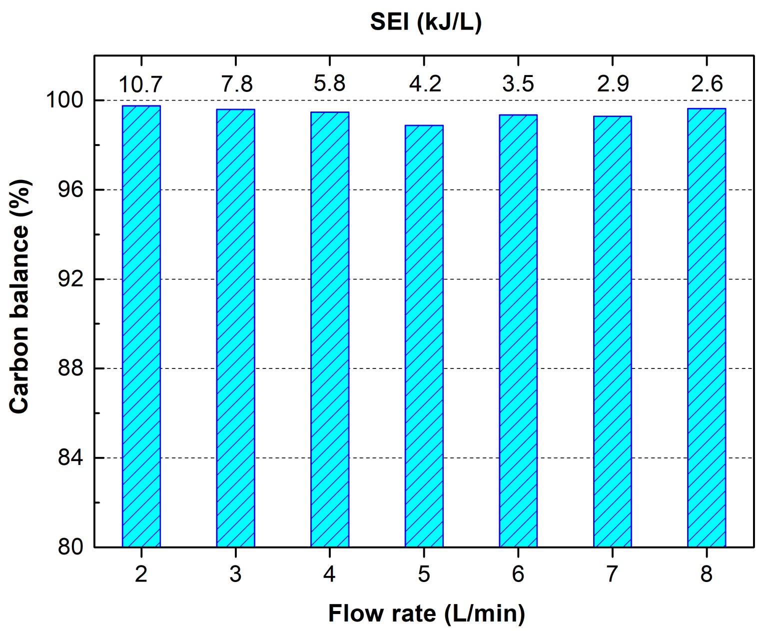

Fig. 4 Carbon balance of the reaction as a function of CO_2 feed flow rate (applied voltage = 10 kV)

As shown in Fig. 4, the carbon balance of the reaction remains at 98.9-99.8% under the studied conditions, indicating that CO was the primary C-containing product in CO_2 dissociation. In addition, the nearly stoichiometric conversion of CO_2 into CO (eq. (1)) was obtained in the plasma processing of CO_2. The missing carbon is probably related to the uncertainty of the measurement. No carbon deposition was found in the experiment. Therefore, in the following sections, the CO_2 conversion and energy efficiency of the plasma process will be considered as the primary indicators of the reaction performance, without focusing on the selectivity and yield of gas products.

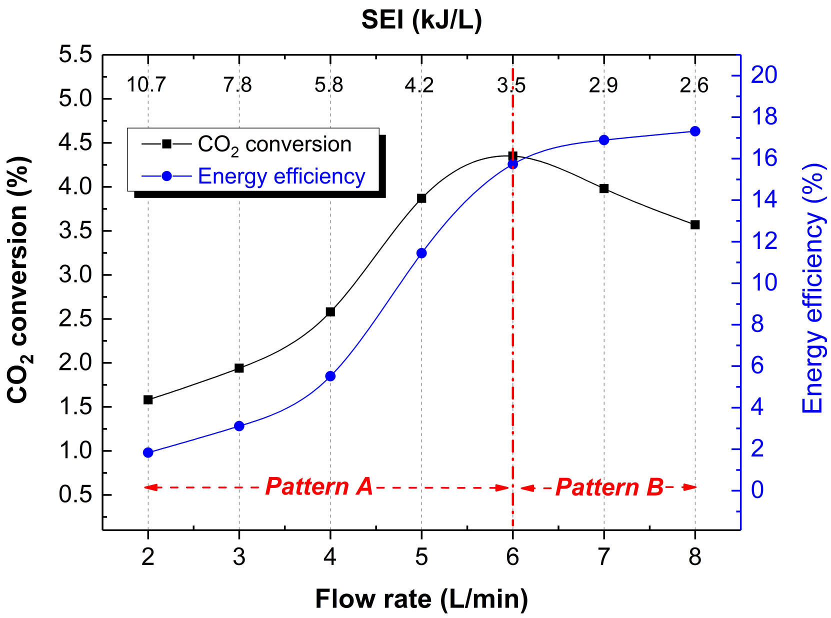

Fig. 5 CO_2 conversion and energy efficiency as a function of feed flow rate and SEI (applied voltage = 10 kV)

Fig. 5 shows that the effect of flow rate and SEI on CO_2 conversion and energy efficiency exhibits two patterns, i.e., Pattern A with flow rates of < 6 L/min (SEI > 3.5 kJ/L) and Pattern B with flow rates of ≥ 6 L/min (SEI ≤ 3.5 kJ/L). The CO_2 conversion initially increases with increasing CO_2 flow rate or decreasing SEI in Pattern A, reaching a maximum of 4.4% at a flow rate of 6 L/min, but followed by a noticeable drop in Pattern B. The energy efficiency shows a continuously rising trend (from 2% to 17%) upon increasing flow rate in both Pattern A and Pattern B but exhibits a slowdown in the increase rate in Pattern B due to the decrease of CO_2 conversion.

It is interesting to note that increasing feed flow rate (and decreasing SEI) increases the conversion of CO_2 in Pattern A. Most of previous studies (e.g., DBD [16, 19, 54], gliding arc plasmatron [31], flat gliding arc discharge [33], and microhollow cathode discharge [55]) showed that increasing feed gas flow rate at a fixed input power had a negative effect on CO_2 conversion due to the decreased retention time of CO_2 in the plasma and the decreased SEI. In addition, a trade-off between the CO_2 conversion and energy efficiency often exists in the plasma decomposition of CO_2, i.e., the increase of CO_2 conversion is always accompanied by a decrease in the energy efficiency. In this study, this commonly reported phenomenon is only found in Pattern B (Fig. 5).

The effect of flow rate on CO_2 conversion shown in Pattern A could be attributed to the combined effect of several factors, i.e., SEI, retention time, gas temperature, and possibly vibrational excitation kinetics. Our previous studies have shown that the RGA plasmas exhibit gas temperatures of 1300-2000 K, which are high enough to promote the recombination of CO and O (eq. (6) [56]), or reverse reaction of eq. (1), indicating that the high temperature of the RGA probably has a detrimental effect on the conversion CO_2. Note that the auto-ignition temperature of CO is around only 878 K and eq. (6) shows that the recombination of CO and O is highly dependent on gas temperature. Sun et al. [29] showed that the conversion of CO_2 and energy efficiency decreased significantly with increasing gas temperature in the range of 1000-1500 K in a gliding arc plasma with knife-shaped electrodes, wherein the recombination between CO and O is the main reaction to limit the conversion of CO_2.

$$\mathrm{CO} + \mathrm{O} \rightarrow \mathrm{CO_2} \qquad k(\mathrm{T}) = 1.7\times10^{-33}[cm^6/molecule^2\,s]\cdot \mathrm{e}^{-12.55\,[kJ/mole]/\mathrm{RT}} \quad (\mathrm{T} = 300 - 2500\mathrm{K}) \quad (6)$$

Where, $k(T)$ refers to the reaction rate constant, T is the gas temperature and R is the universal gas constant.

The measured outlet gas temperature in the experiment is plotted in Fig. 6. A drop of temperature can be observed only in the range of 4 to 6 L/min, where coincidentally the CO_2 conversion and energy efficiency show the highest increase rate (0.9% and 5.1% per L/min, respectively), as clearly shown in Fig. 5. This phenomenon partially manifests that the gas temperature plays a non-negligible opposite role in the conversion of CO_2 due to the recombination of CO and O. In this regard, unlike that in DBD or other reported discharges that normally have lower gas temperature (e.g., <800K), the effect of residence time in the RGA on CO_2 conversion should be negative. In the RGA plasma reactions, fast attainment of steady state ensures a nearly instantaneous dissociation of CO_2 and a longer residence time could induce an opposite effect as the reverse reaction is promoted at such a high temperature. This should be one reason why increasing flow rate in Pattern A increases the CO_2 conversion. The residence time of CO_2 in the plasma area (the ratio of plasma volume to flow rate), declines from 159.2 to 53.1 ms when increasing flow rate from 2 to 6 L/min in Pattern A.

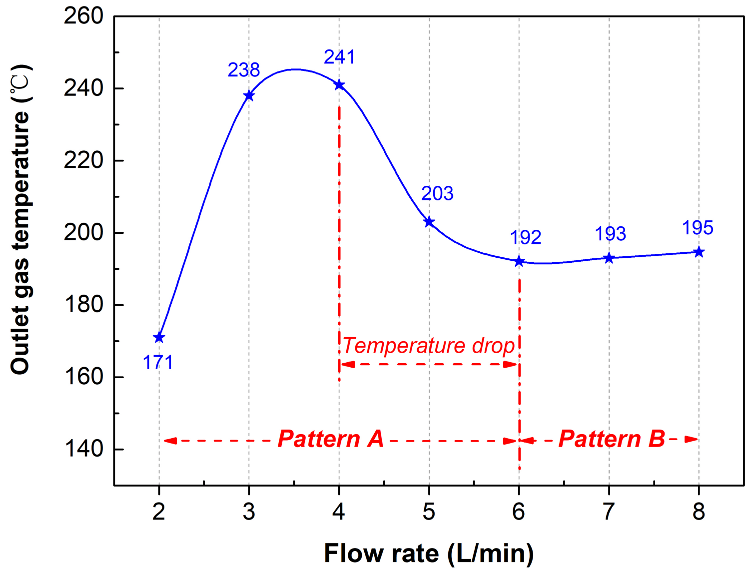

Fig. 6 Effect of CO_2 flow rate on the outlet gas temperature

In addition, our previous study demonstrated that increasing flow rate could enhance the vibrational kinetics energy of the RGA plasma under the studied conditions [57], which probably steers the activation of CO_2 into a more efficient pathway through vibrational excitation and thus improves the CO_2 conversion. In Pattern B, the decrease of CO_2 conversion could be associated with the decrease of SEI, as commonly reported in plasma chemical processes [3].

Kim et al. reported that the flow rate exhibited a similar effect on CO_2 conversion in a gliding arc plasma with knife-shaped electrodes, i.e., the conversion of CO_2 reached a maximum value upon increasing flow rate from 6 L/min to 14 L/min, then decreased when further increasing the flow rate [58]. However, quite different from the reason in this study, this phenomenon was related to the intrinsic property of the flat gliding arc, in which a high flow rate is generally indispensable to push the arc moving along the electrodes and generate an effective plasma zone for chemical reactions. Increasing the gas flow rate from 6 L/min to 14 L/min enlarged the plasma discharge column between the electrodes and thus improved the CO_2 conversion. After reaching a peak value, the CO_2 conversion started to drop because of the decrease in retention time and SEI. Note that, in the RGA reactor, the plasma zone can remain almost the same under the studied feed flow rates. A relatively low flow rate (e.g., 1-2 L/min) is sufficient to sustain a three-dimensional plasma zone and there is no specific requirement for the flow rate, providing the flexibility and adaptability of this process for its practical application.

Based on the results, a CO_2 flow rate of 6-7 L/min is recommended to simultaneously obtain a relatively high CO_2 conversion (4.0-4.4%) and energy efficiency (16-17%) in the RGA system. Compared to other non-thermal plasmas used for CO_2 decomposition, e.g., DBD plasma (CO_2 conversion of 3-33%, energy efficiency of 2-9%) [16, 18, 59, 60] and corona discharge (CO_2 conversion of 3-20%, energy efficiency of 1-10%) [61, 62] the RGA plasma exhibits a slightly lower CO_2 conversion but higher energy efficiency. Importantly, it can allow a feed flow rate (6-7 L/min) of two orders of magnitude higher in comparison to typical DBD and corona discharges (20-125 ml/min), which is favorable for an industrial process. Further enhancement of the reaction performance can be expected by cooling the reactor to lower the gas temperature of the RGA plasma, in order to limit the recombination of CO and O.

3.2 Effect of applied voltage and arc current

The applied voltage and arc current are not only associated with the SEI but also affect the physical characteristics of plasma [53, 63]. Fig. 7 and Fig. 8 illustrate the variation of CO_2 conversion and energy efficiency as a function of applied voltage and arc current, respectively. Increasing applied voltage or arc current decreases the energy efficiency of the plasma process. However, the change of applied voltage and arc current has different effects on the CO_2 conversion. The conversion of CO_2 initially increases with the increase of applied voltage from 5 to 8 kV (SEI from 1.8 to 3.2 kJ/L) and reaches a peak of 4.6% at an applied voltage of 8 kV, followed by a drop to 3.9% when further increasing applied voltage to 10 kV. The decrease of CO_2 conversion with the increase of applied voltage from 8 to 10 kV could be attributed to enhanced recombination of CO and O due to the increased gas temperature. By contrast, the CO_2 conversion increase with increasing the arc current from 50 to 170 mA (SEI from 1.2 to 3.5 kJ/L).

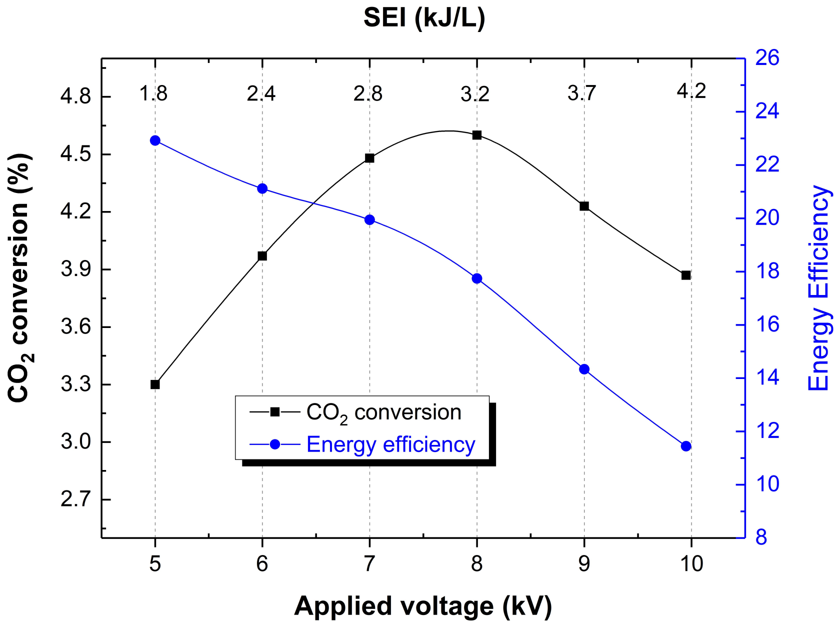

Fig. 7 CO_2 conversion and energy efficiency as a function of applied voltage and SEI

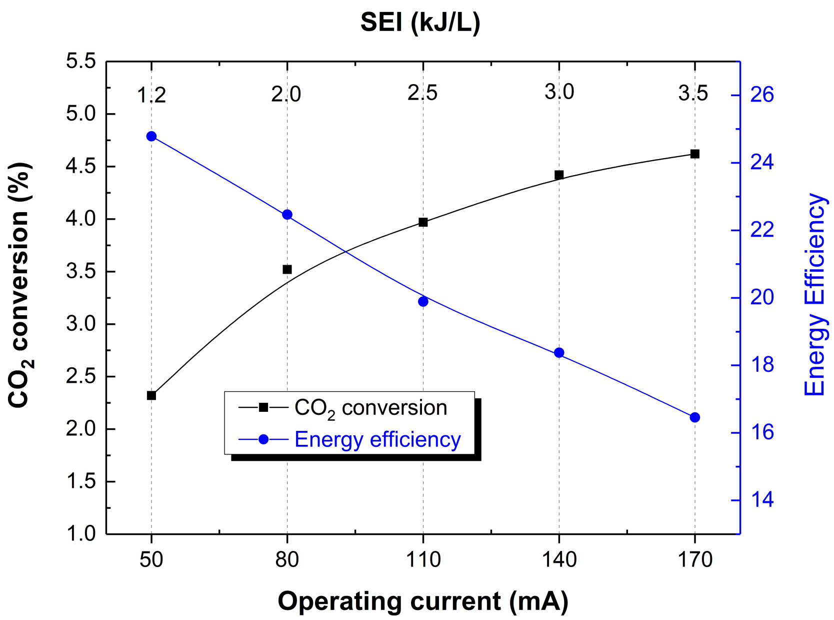

Fig. 8 CO_2 conversion and energy efficiency as a function of arc current (and SEI)

The variation of applied voltage or arc current is related to the change of the SEI. Fig. 9 shows the effect of SEI on the CO_2 conversion and energy efficiency. Again, two different patterns can be clearly observed, i.e., Pattern A with SEI > 3.5 kJ/L and Pattern B with SEI ≤ 3.5 kJ/L. In Pattern A, the CO_2 conversion and energy efficiency increase simultaneously with the decrease of SEI, whereas in Pattern B, a trade-off exists between them, which is well consistent with the results shown in Fig. 5. The above phenomenon indicates that the SEI is a predominant factor in the RGA assisted CO_2

decomposition process.

It should be noted that, the outlet gas temperatures in Pattern A were higher than that in Pattern B except for flow rate of 2 L/min, suggesting that the high-temperature stimulated recombination of CO and O in Pattern A could partly contribute to the decreased CO_2 conversion when increasing the SEI.

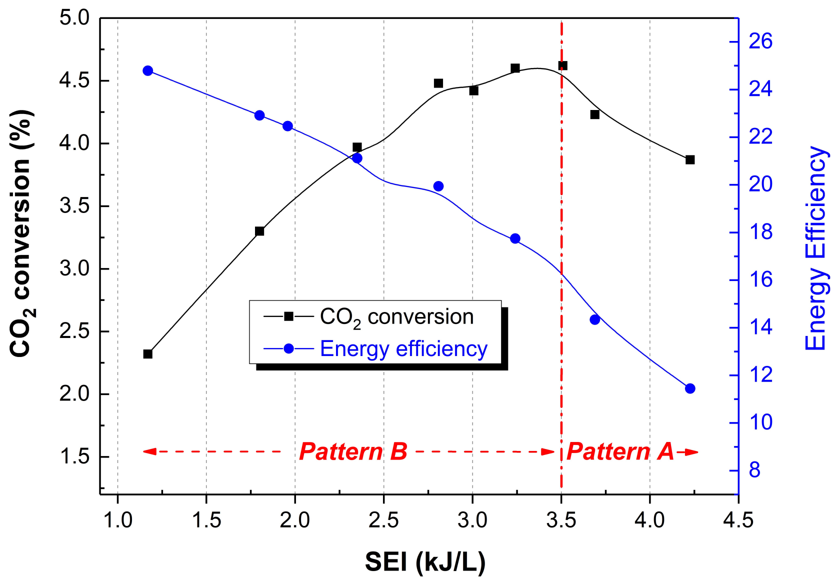

Fig. 9 CO_2 conversion and energy efficiency as a function of SEI

3.3 Effect of additive gases

The effect of additive gas (e.g., N_2, Ar, and He) on the plasma conversion of CO_2 has also been evaluated in previous works, for example, gliding arc discharge in N_2 [33], DBD in N_2, Ar, and He [8, 60, 64-66], glow discharge in He [62, 67], microhollow cathode discharge in Ar [55], microwave discharge in N_2 [68], and radio frequency discharge in Ar [69]. The presence of additive gas in the plasma CO_2 conversion could affect the discharge characteristics, CO_2 conversion, energy efficiency, and even by-product formation in the case of N_2 [3]. In this work, a comparative study of CO_2 dissociation in the RGA plasma using N_2 and Ar as an additive gas was performed (Fig. 10).

Clearly, increasing N_2 and Ar concentration from around 10% to 95% enhances the CO_2 conversion, i.e., from 2.8% to 12.7% and from 2.8% to 10.6%, respectively. Interestingly, a faster increase rate of CO_2 conversion can be observed when the N_2 or Ar concentration is higher than 70%. This positive effect of additive gas on CO_2 dissociation can be attributed to the increased dissociation pathways of CO_2 due to the formation of excited N_2 or Ar species. Although Ar is easier to be ignited in plasma, N_2 is more beneficial for enhancing the CO_2 conversion in comparison to Ar in this work. The CO_2 conversion and the energy efficiency (and also the SEI) in N_2 are both higher than those of Ar, particular at an additive gas concentration of 60-70% (107-119% and 82-93% higher, respectively). Similar results were also reported using a pulse DBD plasma [66].

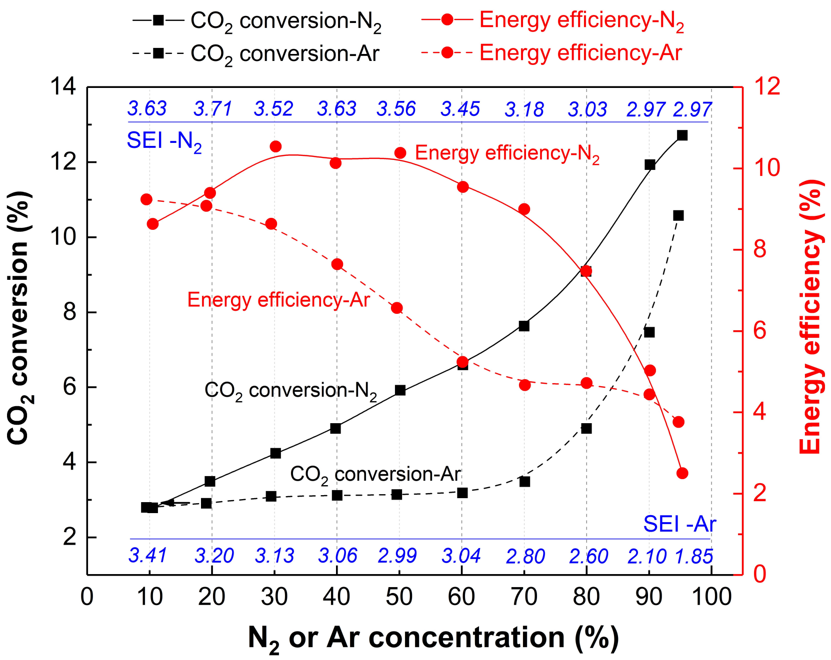

Fig. 10 Effect of additive gases (N_2 and Ar) on the CO_2 conversion and energy efficiency (total flow rate = 5.9 L/min, applied voltage = 10 kV)

This phenomenon can be resulted from the following two aspects. Firstly, upon adding N_2, excited N_2 metastable molecules, e.g., $N_2(A)$ and $N_2(a')$, can be formed due to the electron-impact processes, which provides more reaction routes for CO_2 conversion in comparison to Ar. For Ar, only limited excited species can be produced (e.g., Ar^*) [8, 33, 68]. The metastable N_2 stimulated CO_2 dissociation is considered as significantly efficient. For example, a modeling study of a CO_2/N_2 DBD plasma revealed that, the reaction of metastable $N_2(A)$ molecule with CO_2 gradually became a dominant pathway for CO_2 dissociation (with contribution of over 45%) when the N_2 concentration was higher than 70% [8]. Secondly, as a diatomic molecule, N_2 has a larger collision cross section compared to Ar, a monoatomic species, thus has a higher probability to collide with CO_2 molecules [66]. It is interesting to note that, in our previous study of RGA assisted methanol decomposition [37], the N_2 plasma also showed significantly better performance compared to Ar RGA in terms of reactant conversion, product selectivity, and energy yield of H_2.

However, the addition of N_2 can result in the formation of unwanted harmful compounds, i.e., N_2O and NO_x compounds (60-1200 ppm in total) [8]. In a detailed modeling work of Snoeckx et al. [8], potential solutions to limit the formation of these harmful compounds were proposed.

To our knowledge, a weakly negative effect of N_2 on CO_2 conversion was reported only in a DBD plasma [65], where the addition of N_2 into CO_2 (CO_2/N_2 molar ratio = 1:1) slightly decreased the CO_2 conversion from 16.1% to 15.4% (total flow rate = 20 ml/min, input power = 15.0 W). The authors attributed this phenomenon to the dissipation of input power due to the N_2 excitation processes when the N_2 concentration and input power were relatively low.

In contrast to the CO_2 conversion, the energy efficiency of the plasma process drops with rising N_2 or Ar fraction (Figure 10), which is in line with other reports [3, 8, 68]. An exception appears in Fig. 9 with an SEI of higher than 3.5 kJ/L (N_2 concentration < 50%), where the energy efficiency slightly increases with increasing N_2 concentration. Remarkably, the turning point of SEI in this case (3.5 kJ/L) is surprisingly the same with that for Pattern A and Pattern B as above discussed.

It should be noted that the energy loss in the ballast resistance that used in the electric circuit was not considered in the calculation of the energy efficiency, which is commonly used in previous works [70, 71]. Ballast resistance is usually used in DC non-thermal arc discharge reactors to limit the discharge current [70, 72-74]. The circuit with a ballast resistance is not optimal from the point of technical application because a large fraction of supplied power could be consumed in the resistance. For instance, if the energy loss in the ballast resistance is taken into account, the energy efficiency for CO_2 conversion in this work can be reduced by around 80%. However, the ballast resistance provides the possibility to operate at a prescribed current value, benefiting the physical investigation and analysis of the obtained data [73]. The elimination of the use of ballast resistance for the improvement of the energy efficiency can be expected by equipping a RGA reactor with two power sources, i.e., a high voltage generator (e.g., 10 kV) to ignite the discharge and a second low voltage power source (e.g., 1 kV) to maintain the discharge [35].

4. Conclusions

In this work, the conversion of CO_2 to CO has been carried out in a DC rotating gliding arc (RGA) warm plasma. The effect of CO_2 flow rate, applied voltage, and arc current on the performance of this process has been investigated, with specific emphasis on the understanding of the role of SEI in the plasma process. In addition, N_2 and Ar are added into the RGA CO_2 plasma to evaluate the effect of the additive gases on the reaction performance.

The influence of flow rate and SEI on CO_2 conversion and energy efficiency shows two different patterns: Pattern A with flow rates of < 6 L/min (SEI > 3.5 kJ/L) and Pattern B with flow rates of ≥ 6 L/min (SEI ≤ 3.5 kJ/L). The CO_2 conversion initially increases with the flow rate (Pattern A), reaching a peak at 6 L/min and then followed by a noticeable drop when further increasing the flow rate to 10 L/min (Pattern B). SEI has been identified as a predominant factor in the RGA CO_2 decomposition process. The presence of two patterns is related to the balance between the conversion of CO_2 and the reverse reaction (recombination of CO and O), both affected by the SEI.

A flow rate of 6-7 L/min is recommended to simultaneously obtain a relatively high CO_2 conversion (4.0-4.4%) and energy efficiency (16-17%) in the RGA system. Remarkably, compared to other commonly studied non-thermal plasmas, the RGA plasma shows significant advantages in processing capacity (feed flow rate). It is expected that, cooling the plasma area to lower the gas temperature could facilitate the CO_2 activation in the RGA plasma, due to the limited recombination of CO and O.

Increasing N_2 and Ar concentration from around 10% to 95% enhances the CO_2 conversion, i.e., from 2.8% to 12.7% and 2.8% to 10.6%, respectively. Compared to Ar, N_2 is shown to be more favorable for CO_2 activation in terms of both CO_2 conversion and energy efficiency due to the formation of more reaction routes for CO_2 conversion.

Acknowledgements

This work is supported by the National Natural Science Foundation of China (No. 51706204 and No. 51576174) and the Science Fund for Creative Research Groups of the National Natural Science Foundation of China (No. 51621005).

References

[1] Pachauri RK, Allen MR, Barros V, Broome J, Cramer W, Christ R, Church J, Clarke L, Dahe Q, Dasgupta P. Climate change 2014: synthesis Report. Contribution of working groups I, II and III to the fifth assessment report of the intergovernmental panel on climate change, IPCC2014.

[2] Saeidi S, Amin NAS, Rahimpour MR. Hydrogenation of CO_2 to value-added products—A review and potential future

developments. J CO_2 Util 2014; 5: 66-81.
[3] Snoeckx R, Bogaerts A. Plasma technology–a novel solution for CO_2 conversion? Chem Soc Rev 2017; 46: 5805-5863.
[4] Banerjee A, Dick GR, Yoshino T, Kanan MW. Carbon dioxide utilization via carbonate-promoted C–H carboxylation, Nature 2016; 531: 215-219.
[5] Mei DH, Zhu XB, He YL, Yan JD, Tu X. Plasma-assisted conversion of CO_2 in a dielectric barrier discharge reactor: understanding the effect of packing materials. Plasma Sources Sci T 2014; 24: 015011.
[6] Wang WZ, Berthelot A, Kolev S, Tu X, Bogaerts A. CO_2 conversion in a gliding arc plasma: 1D cylindrical discharge model. Plasma Sources Sci T 2016; 25: 065012.
[7] Lahijani P, Zainal ZA, Mohammadi M, Mohamed AR. Conversion of the greenhouse gas CO_2 to the fuel gas CO via the Boudouard reaction: A review. Renew Sust Energ Rev 2015; 41: 615-632.
[8] Snoeckx R, Heijkers S, Van Wesenbeeck K, Lenaerts S, Bogaerts A. CO_2 conversion in a dielectric barrier discharge plasma: N_2 in the mix as a helping hand or problematic impurity? Energ Environ Sci 2016; 9: 999-1011.
[9] Mei DH, Zhu XB, Wu CF, Ashford B, Williams PT, Tu X. Plasma-photocatalytic conversion of CO_2 at low temperatures: Understanding the synergistic effect of plasma-catalysis. Appl Catal B- Environ 2016; 182: 525-532.
[10] Fridman A. Plasma chemistry. New York: Cambridge University Press; 2008.
[11] Liu SY, Mei DH, Wang L, Tu X. Steam reforming of toluene as biomass tar model compound in a gliding arc discharge reactor. Chemi Eng J 2017; 307: 793-802.
[12] Zhu JJ, Ehn A, Gao J, Kong C, Aldén M, Salewski M, Leipold F, Kusano Y, Li ZS. Translational, rotational, vibrational and electron temperatures of a gliding arc discharge. Opt. Express 2017; 25: 20243-20257.
[13] Gangoli SP, Gutsol AF, Fridman AA. A non-equilibrium plasma source: magnetically stabilized gliding arc discharge: I. Design and diagnostics. Plasma Sources Sci T 2010; 19: 065003.
[14] Fridman AA, Gutsol AF, Gangoli SP, Ju Y, Ombrello T. Characteristics of gliding arc and its application in combustion enhancement. J Propul Power 2008; 24: 1216-1228.
[15] Snoeckx R, Ozkan A, Reniers F, Bogaerts A. The quest for value-added products from carbon dioxide and water in a dielectric barrier discharge: A chemical kinetics study. ChemSusChem 2016; 10: 409-424.
[16] Mei DH, Tu X. Conversion of CO_2 in a cylindrical dielectric barrier discharge reactor: Effects of plasma processing parameters and reactor design. J CO_2 Util 2017; 19: 68-78..
[17] Wang L, Yi YH, Guo HC, Tu X. Atmospheric pressure and room temperature synthesis of methanol through plasma-catalytic hydrogenation of CO_2. ACS Catal 2018; 8: 90-100.
[18] Aerts R, Somers W, Bogaerts A. Carbon dioxide splitting in a dielectric barrier discharge plasma: a combined experimental and computational study. ChemSusChem 2015; 8: 702-716.
[19] Ozkan A, Bogaerts A, Reniers F. Routes to increase the conversion and the energy efficiency in the splitting of CO_2 by a dielectric barrier discharge. J Phys D Appl Phys 2017; 50: 084004.
[20] Brehmer F, Welzel S, Van De Sanden M, Engeln R. CO and byproduct formation during CO_2 reduction in dielectric barrier discharges. J Appl Phys 2014; 116: 123303.
[21] Michielsen I, Uytdenhouwen Y, Pype J, Michielsen B, Mertens J, Reniers F, Meynen V, Bogaerts A. CO_2 dissociation in a packed bed DBD reactor: First steps towards a better understanding of plasma catalysis. Chem Eng J 2017; 326: 477-488.
[22] Wang WZ, Mei DH, Tu X, Bogaerts A. Gliding arc plasma for CO_2 conversion: better insights by a combined experimental and modelling approach. Chem Eng J 2017; 330: 11-25.
[23] Butterworth T, Elder R, Allen R. Effects of particle size on CO_2 reduction and discharge characteristics in a packed bed plasma reactor. Chem Eng J 206; 293: 55-67.
[24] Van Rooij G, van den Bekerom D, den Harder N, Minea T, Berden G, Bongers W, Engeln R, Graswinckel M, Zoethout E, van de Sanden M. Taming microwave plasma to beat thermodynamics in CO_2 dissociation. Faraday Discuss 2015; 183: 233-248.

[25] Bongers W, Bouwmeester H, Wolf B, Peeters F, Welzel S, van den Bekerom D, den Harder N, Goede A, Graswinckel M, Groen PW. Plasma-driven dissociation of CO_2 for fuel synthesis. Plasma Process Polym 2017; 14.
[26] Spencer L, Gallimore A. CO_2 dissociation in an atmospheric pressure plasma/catalyst system: a study of efficiency, Plasma Sources Sci T 2012; 22: 015019.
[27] Silva T, Britun N, Godfroid T, Snyders R. Optical characterization of a microwave pulsed discharge used for dissociation of CO_2. Plasma Sources Sci T 2014; 23: 025009.
[28] Chen G, Georgieva V, Godfroid T, Snyders R, Delplancke-Ogletree MP. Plasma assisted catalytic decomposition of CO_2. Appl Catal B- Environ 2016; 190: 115-124.
[29] Sun S, Wang H, Mei D, Tu X, Bogaerts A, CO_2 conversion in a gliding arc plasma: Performance improvement based on chemical reaction modeling. J CO2 Util 2017; 17: 220-234.
[30] Nunnally T, Gutsol K, Rabinovich A, Fridman A, Gutsol A, Kemoun A. Dissociation of CO_2 in a low current gliding arc plasmatron. J Phys D Appl Phys 2011; 44: 274009.
[31] Ramakers M, Trenchev G, Heijkers S, Wang WZ, Bogaerts A. Gliding Arc Plasmatron: providing an alternative method for carbon dioxide conversion. ChemSusChem 2017; 10: 2642-2652.
[32] Indarto A, Choi JW, Lee H, Song HK. Conversion of CO_2 by gliding arc plasma. Environ Eng Sci 2006; 23: 1033-1043.
[33] Indarto A, Yang DR, Choi JW, Lee H, Song HK. Gliding arc plasma processing of CO_2 conversion. J Hazard Mater 2007; 146: 309-315.
[34] Liu JL, Park HW, Chung WJ, Park DW. High-efficient conversion of CO_2 in AC-pulsed tornado gliding arc plasma. Plasma Chem Plasma P 2016; 36: 437-449.
[35] Fridman A, Nester S, Kennedy LA, Saveliev A, Mutaf-Yardimci O. Gliding arc gas discharge. Prog Energ Combust. 1999; 25: 211-231.
[36] Kusano Y., Sørensen BF, Andersen TL, Toftegaard HL, Leipold F, Salewski M, Sun Z, Zhu J, Li Z, Alden M. Water-cooled non-thermal gliding arc for adhesion improvement of glass-fibre-reinforced polyester, J Phys D Appl Phys 2013; 46: 135203.
[37] Zhang H, Li XD, Zhu FS, Bo Z, Cen KF, Tu X, Non-oxidative decomposition of methanol into hydrogen in a rotating gliding arc plasma reactor. Int J Hydrogen Energ 2015; 40: 15901-15912.
[38] Zhang H, Zhu FS, Bo Z, Cen KF, Li XD. Hydrogen production from methanol decomposition in a gliding arc discharge plasma with high processing capacity. Chem Lett 2015; 44: 1315-1317.
[39] Zhu J, Sun Z, Li Z, Ehn A, Aldén M, Salewski M, Leipold F, Kusano Y. Dynamics, OH distributions and UV emission of a gliding arc at various flow-rates investigated by optical measurements. J Phys D Appl Phys 2014; 47: 295203.
[40] Sun Z, Zhu J, Li Z, Aldén M, Leipold F, Salewski M, Kusano Y. Optical diagnostics of a gliding arc, Opt Express 2013; 21; 6028-6044.
[41] Zhu J, Gao J, Ehn A. Aldén M, Li Z, Moseev D, Kusano Y, Salewski M, Alpers A, Gritzmann P. Measurements of 3D slip velocities and plasma column lengths of a gliding arc discharge. Appl Phys Lett 2015; 106: 044101.
[42] Zhang H, Zhu FS, Li XD, Cen KF, Du CM, Tu X. Enhanced hydrogen production by methanol decomposition using a novel rotating gliding arc discharge plasma. RSC Adv 2016; 6: 12770-12781.
[43] Zhang H, Li XD, Zhang YQ, Chen T, Yan JH, Du CM. Rotating gliding arc codriven by magnetic field and tangential flow, IEEE Tran Plasma Sci 2012; 40: 3493-3498.
[44] Zhang H, Du CM, Wu AJ, Bo Z, Yan JH, Li XD. Rotating gliding arc assisted methane decomposition in nitrogen for hydrogen production. Int J Hydrogen Energ 2014; 39: 12620-12635.
[45] Lee D, Kim KT, Cha M, Song YH. Optimization scheme of a rotating gliding arc reactor for partial oxidation of methane. P Combust Inst 2007; 31: 3343-3351.
[46] Lee D, Kim KT, Kang HS, Jo S, Song YH. Optimization of NH 3 decomposition by control of discharge mode in a rotating arc. Plasma Chem Plasma P 2014; 34: 111-124.

[47] Ombrello T, Qin X, Ju Y, Gutsol AF, Fridman AA, Carter C. Combustion enhancement via stabilized piecewise nonequilibrium gliding arc plasma discharge. AIAA J 2006; 44: 142-150.
[48] Zhang H, Zhu FS, Li XD, Cen KF, Du CM, Tu X. Rotating gliding arc assisted water splitting in atmospheric nitrogen. Plasma Chem Plasma P 2016; 36: 813-834.
[49] Stanfield SA, Menart J, DeJoseph Jr C, Kimmel RL, Hayes JR. Rotational and vibrational temperature distributions for a dielectric barrier discharge in air. AIAA J 2009; 47: 1107.
[50] Masoud N, Martus K, Figus M, Becker K. Rotational and vibrational temperature measurements in a high-pressure cylindrical dielectric barrier discharge (C-DBD). Contrib Plasm Phys 2005; 45: 32-39.
[51] Zhang S, Wang W, Jia L, Liu Z, Yang Y, Dai L. Rotational, vibrational, and excitation temperatures in bipolar nanosecond-pulsed diffuse dielectric-barrier-discharge plasma at atmospheric pressure. IEEE Tran Plasma Sci 2013; 41: 350-354.
[52] Tu X, Gallon HJ, Whitehead JC. Electrical and spectroscopic diagnostics of a single-stage plasma-catalysis system: effect of packing with TiO_2. J Phys D Appl Phys 2011; 44: 482003.
[53] Zhang H, Zhu FS, Tu X, Bo Z, Cen KF, Li XD. Characteristics of atmospheric pressure rotating gliding arc plasmas. Plasma Sci Technol 2016; 18: 473.
[54] Paulussen S, Verheyde B, Tu X, De Bie C, Martens T, Petrovic D, Bogaerts A, Sels B. Conversion of carbon dioxide to value-added chemicals in atmospheric pressure dielectric barrier discharges. Plasma Sources Sci T 2010; 19: 034015.
[55] Taylan O, Berberoglu H. Dissociation of carbon dioxide using a microhollow cathode discharge plasma reactor: effects of applied voltage, flow rate and concentration. Plasma Sources Sci T 2014; 24: 015006.
[56] Tsang W, Hampson R. Chemical kinetic data base for combustion chemistry. Part I. Methane and related compounds, J Phys Chem Ref Data 1986; 15: 1087-1279.
[57] Wu AJ, Zhang H, Li XD, Lu SY, Du CM, Yan JH. Determination of spectroscopic temperatures and electron density in rotating gliding arc discharge. IEEE Tran Plasma Sci 2015; 43: 836-845.
[58] Kim SC, Lim MS, Chun YN. Reduction characteristics of carbon dioxide using a plasmatron. Plasma Chem Plasma P 2014; 34: 125-143.
[59] Mei DH, Tu X. Atmospheric pressure non-thermal plasma activation of CO_2 in a packed-bed dielectric barrier discharge reactor. ChemPhysChem 2017; 18: 3253-3259.
[60] Duan X, Li Y, Ge W, Wang B. Degradation of CO_2 through dielectric barrier discharge microplasma. Greenhouse Gases 2015; 5: 131-140.
[61] Xu W, Li MW, Xu GH, Tian YL. Decomposition of CO_2 using DC corona discharge at atmospheric pressure. Jpn J Appl Phys 2004; 43: 8310.
[62] Wang JY, Xia GG, Huang A, Suib SL, Hayashi Y, Matsumoto H. CO_2 decomposition using glow discharge plasmas. J Catal 1999; 185: 152-159.
[63] Zhang H, Zhu FS, Li XD, Du CM. Dynamic behavior of a rotating gliding arc plasma in nitrogen: effects of gas flow rate and operating current. Plasma Sci Technol 2017; 19: 045401.
[64] Yap D, Tatibouët JM, Batiot-Dupeyrat C. Carbon dioxide dissociation to carbon monoxide by non-thermal plasma. J CO_2 Util 2015; 12: 54-61.
[65] Duan XF. Carbon dioxide decomposition with dielectric barrier discharge microplasma. Master thesis. Tianjin: Tianjin University; 2015 (in Chinese).
[66] Wang T, Liu H, Xiong X, Feng X. Conversion of carbon dioxide to carbon monoxide by pulse dielectric barrier discharge plasma. IOP Conference Series: Earth and Environmental Science, IOP Publishing, 2017, pp. 012100.
[67] Brock SL, Shimojo T, Marquez M, Marun C, Suib SL, Matsumoto H, Hayashi Y. Factors influencing the decomposition of CO 2 in AC fan-type plasma reactors: Frequency, waveform, and concentration effects. J Catal 1999; 184: 123-133.
[68] Heijkers S, Snoeckx R, Kozák TS, Silva T, Godfroid T, Britun N, Snyders R, Bogaerts A. CO_2 conversion in a

microwave plasma reactor in the presence of N_2: elucidating the role of vibrational levels. J Phys Chem C 2015; 119: 12815-12828.
[69] Spencer LF, Gallimore AD. Efficiency of CO_2 dissociation in a radio-frequency discharge. Plasma Chem Plasma P 2011; 31: 79-89.
[70] Yu L, Tu X, Li X, Wang Y, Chi Y, Yan J. Destruction of acenaphthene, fluorene, anthracene and pyrene by a dc gliding arc plasma reactor. J Hazard Mater 2010; 180: 449-455.
[71] Yu L, Li X, Tu X, Wang Y, Lu S, Yan J, Decomposition of naphthalene by dc gliding arc gas discharge. J Phys Chem C 2009; 114: 360-368.
[72] Korolev YD, Frants OB, Landl NV, Geyman VG, Karengin AG, Pobereznikov AD, Kim Y, Rosocha LA, Matveev IB. Plasma-assisted combustion system for incineration of oil slimes. IEEE Trans Plasma Sci 2013; 41: 3214-3222.
[73] Korolev YD, Frants OB, Landl NV, Geyman VG, Matveev IB. Glow-to-spark transitions in a plasma system for ignition and combustion control. IEEE Trans Plasma Sci 2007; 35: 1651-1657.
[74] Janda M, Morvova M, Machala Z, Morva I. Study of plasma induced chemistry by DC discharges in $CO_2/N_2/H_2O$ mixtures above a water surface. Origins Life and Evol B 2008; 38: 23-35.